Received: 26 October 2023 | Accepted: 17 December 2023

DOI: 10.1111/1365-2435.14518

Functional Ecology | BRITISH ECOLOGICAL SOCIETY

RESEARCH ARTICLE

Pushing the limits of C_3 intrinsic water use efficiency in Mediterranean semiarid steppes: Responses of a drought-avoider perennial grass to climate aridification

Wei Ren[1,2,3] | Pablo García-Palacios[4] | Santiago Soliveres[5,6] | Iván Prieto[1,7] | Fernando T. Maestre[5,6] | José Ignacio Querejeta[1]

[1]Centro de Edafología y Biología Aplicada del Segura, Consejo Superior de Investigaciones Científicas (CEBAS, CSIC), Murcia, Spain; [2]Chongqing Key Laboratory of Karst Environment, School of Geographical Sciences, Southwest University, Chongqing, China; [3]Institute of International Rivers and Eco-Security, Yunnan University, Kunming, China; [4]Instituto de Ciencias Agrarias, Consejo Superior de Investigaciones Científicas, Madrid, Spain; [5]Instituto Multidisciplinar para el Estudio del Medio "Ramon Margalef", Universidad de Alicante, Alicante, Spain; [6]Departamento de Ecología, Universidad de Alicante, Alicante, Spain and [7]Departamento de Biodiversidad y Gestión Ambiental, Universidad de León, León, Spain

Correspondence
José Ignacio Querejeta
Email: querejeta@cebas.csic.es

Funding information
Spanish Ministry of Science and Innovation, Grant/Award Number: EUR2022-134048, PRX19/00301, PID2019-107382RB-I00, CGL2013-48753-R, CGL2010-21064, AGL-2006-11234, PID2020-113021RA-I00, RTI2018-098895-A-100 and RYC-2016-20604; Fundación BBVA, Grant/Award Number: BIOCON06/105; Universidad Rey Juan Carlos, Grant/Award Number: URJC-RNT-063-2; European Research Council, Grant/Award Number: 647038; Generalitat Valenciana, Grant/Award Number: CIDEGENT/2018/041; National Natural Science Foundation of China, Grant/Award Number: 41801091; China Postdoctoral Science Foundation, Grant/Award Number: 2018M643542 and 2019T120868; Fundación Séneca, Grant/Award Number: 20654/JLI/18

Handling Editor: Antonella Gori

Abstract

1. Intrinsic water use efficiency (WUEi) reflects the trade-off between photosynthetic carbon gain and water loss through stomatal conductance and is key for understanding dryland plant responses to climate change. *Stipa tenacissima* is a perennial tussock C_3 grass with an opportunistic, drought-avoiding water use strategy that dominates arid and semiarid steppes across the western Mediterranean region. However, its ecophysiological responses to aridification and woody shrub encroachment, a major land-use change in drylands worldwide, are not well-understood.
2. We investigated the variations in leaf stable isotopes ($\delta^{18}O$, $\delta^{13}C$, $\delta^{15}N$), nutrient concentrations (N, P, K), and culm water content and isotopic composition ($\delta^{18}O$, $\delta^{2}H$) of paired pure-grass and shrub-encroached *S. tenacissima* steppes along a 350 km aridity gradient in Spain (10 sites, 160 individuals).
3. Culm water isotopes revealed that *S. tenacissima* is a shallow-rooted grass that depends heavily on recent rainwater for water uptake, which may render it vulnerable to increasingly irregular rainfall combined with faster topsoil drying under climate warming and aridification. With increasing aridity, *S. tenacissima* enhanced leaf-level WUE_i through more stringent stomatal regulation of plant water flux and carbon assimilation (higher $\delta^{13}C$ and $\delta^{18}O$), reaching exceptionally high $\delta^{13}C$ values (−23‰ to −21‰) at the most arid steppes. Foliar N concentration was remarkably low across sites regardless of woody shrub encroachment, evidencing severe water and N co-limitation of photosynthesis and productivity. Shrub encroachment decreased leaf P and K but did not affect *S. tenacissima* water status. Perennial grass cover decreased markedly with both declining winter rainfall

and shrub encroachment suggesting population-level rather than individual-level responses of *S. tenacissima* to these changes.

4. The fundamental physiological constraints of photosynthetic C_3 metabolism combined with low foliar N content may hamper the ability of *S. tenacissima* and other drought-avoider species with shallow roots to achieve further adaptive improvements in WUE_i under increasing climatic stress. A drought-avoiding water use strategy based on early stomatal closure and photosynthesis suppression during prolonged rainless periods may thus compromise the capacity of semiarid *S. tenacissima* steppes to maintain perennial grass cover, sustain productivity and cope with ongoing climate aridification at the drier parts of their current distribution.

KEYWORDS
climate aridification, drought avoidance, drylands, foliar nutrients, intrinsic water use efficiency, *Stipa tenacissima*, stomatal regulation, water and nitrogen co-limitation

1 | INTRODUCTION

Climate projection models for the Mediterranean region predict large increases in temperature and vapour pressure deficit (VPD), along with reductions in the amount and regularity of precipitations (Giorgi & Lionello, 2008). Climate aridification will thus increase heat and drought stress, with potentially negative consequences for native vegetation cover, productivity, and persistence in the warmest and driest parts of the Mediterranean biome (Guiot & Cramer, 2016). A better understanding of how changes in temperature and water availability along aridity gradients modulate the physiological performance of native plants is needed to better predict species responses to ongoing climate change in Mediterranean drylands (Prentice et al., 2011; Stewart et al., 1995; Wang et al., 2016).

Dryland plants must endure frequent drought spells in combination with extremely high temperatures causing severe water and heat stress. Levitt (1980) defined different "functional strategies" that plant species can adopt to cope with drought, such as avoidance or tolerance (Peguero-Pina et al., 2020). Co-occurring dryland plants often differ markedly in their water use strategies and tolerance to drought stress (Moreno-Gutiérrez et al., 2012; Pivovaroff et al., 2016). Species with a drought-avoidance strategy are characterised by early stomatal closure before any large decline in plant water potential occurs, whereas drought-tolerant species exhibit simultaneous decreases in stomatal conductance and water potential (Martínez-Ferri et al., 2000). In drought-tolerant species, drought-induced stomatal closure is gradual and allows the maintenance of substantial carbon assimilation during prolonged drought. In contrast, early stomatal closure during drought hampers carbon assimilation and photosynthesis in drought-avoiders. This key difference in the ability of drought-avoider and drought-tolerant species to maintain a net carbon assimilation under water stress suggests that predicted climate aridification may impose very different restrictions on photosynthesis and plant carbon balance between them in drylands where climate change will further shorten and already short growing season. Yet, the limits and constraints of the drought-avoidance strategy, or how it is affected by co-occurring land-cover changes are not well-understood.

Arid and semiarid steppes dominated by the perennial tussock grass *Stipa tenacissima* L. are a dominant vegetation type across the drier parts of the western Mediterranean region, where they occupy around 2.8 million ha (Le Houérou, 2001). These semiarid steppes have a long and complex human management history linked to economic exploitation of *S. tenacissima* fibre since ancient times. *S. tenacissima* is a typical drought-avoider species that shows opportunistic physiological activity and growth after isolated rainfall events (rain-pulses; Pugnaire et al., 1996; Sánchez-Martín et al., 2021). This species exhibits a rapid increase in stomatal conductance, photosynthesis, and green leaf biomass after rainy events when topsoil moisture reaches adequate levels (Haase et al., 1999; Pugnaire & Haase, 1996). *S. tenacissima* closes stomata early when topsoil moisture decreases, rolls-in leaves and conceals the stomata in leaf grooves that become deeper with leaf dehydration to minimise water losses, which drastically reduces transpiration and carbon assimilation (Balaguer et al., 2002; Ramírez et al., 2008, 2009). Genetic differentiation among *S. tenacissima* populations from different climatic regions suggest that both phenotypic physiological plasticity and genetic differentiation may control their responses to climate change (Krichen et al., 2022). Semiarid *S. tenacissima* steppes are undergoing further aridification with anthropogenic climate change (Mariem & Chaieb, 2017) and are experiencing extensive woody shrub encroachment (Maestre et al., 2009), a major land-cover change occurring in many dryland regions worldwide (Eldridge et al., 2011). However, it remains unknown whether (or how) shrub encroachment influences the responses of native perennial grasses to key climate change drivers including aridification.

Intrinsic water use efficiency (WUEi), which is determined by the ratio between photosynthesis and stomatal conductance, is an indicator of the trade-off between carbon gain and water loss at leaf level and thus is a key trait for understanding plant responses to

climate change (Kannenberg et al., 2021). Dryland plants often show higher leaf N concentrations than species from wetter environments as an adaptive trait to enhance their carboxylation capacity and WUEi at any given stomatal conductance to save water during photosynthesis (Wright et al., 2001, 2003). Thus, increasing N allocation to foliar tissues could be an adaptive response to drought stress along aridity gradients to maintain carbon assimilation and increase WUEi while reducing water losses (Grossiord et al., 2018). However, reductions in moisture associated to increases in aridity also reduce nutrient diffusion and mobility in drier soils (Querejeta, Ren, et al., 2021a). Tighter stomatal regulation of plant water flux in response to increasing drought stress further reduces transpiration-driven mass flow of nutrients to roots (Cramer et al., 2009). Climate warming and drying can also impair soil nutrient acquisition by roots and their symbiotic mycorrhizal fungi (Alguacil et al., 2022; León-Sánchez et al., 2018, 2020; Querejeta, Schlaeppi, et al., 2021), and hamper soil nutrient cycling and nutrient resorption from senescing leaves (Prieto & Querejeta, 2020). All of the above could exacerbate the nitrogen co-limitation of primary productivity along aridity gradients. Increasing water and nitrogen co-limitation of photosynthesis with aridity might thus hamper or prevent any adaptive improvements in carboxylation capacity and WUEi through enhanced foliar N contents. However, few studies have examined this question in detail so far (Khasanova et al., 2013).

The stable carbon, oxygen and nitrogen isotope composition of plant leaves can provide insight into the major environmental factors constraining plant ecophysiological performance and nutrition in dryland ecosystems. Leaf $\delta^{13}C$ provides a useful proxy index for assessing time-integrated WUEi (Cernusak et al., 2013). Progressive stomatal closure with drought stress causes a proportionally smaller decrease in photosynthesis than in stomatal conductance, and thus increases both WUEi and $\delta^{13}C$. The simultaneous measurement of $\delta^{13}C$ and $\delta^{18}O$ in leaves helps to separate the independent effects of photosynthesis and stomatal conductance on $\delta^{13}C$, given that $\delta^{18}O$ shares dependence on stomatal conductance with $\delta^{13}C$, but is unaffected by photosynthesis (Barbour, 2007; Querejeta et al., 2007; Scheidegger et al., 2000). Leaf $\delta^{15}N$ integrates the net effects of a wide range of factors including climate, soil fertility, the isotopic signature of soil N pools, the interplay between changes in soil N availability and plant demand, and root mycorrhizal association types (Ruiz-Navarro et al., 2016 and references therein). Stable isotopes offer the key advantage of providing time-integrated information on plant physiological activity over the entire period when the leaves were formed, compared to other conventional methods that can only provide snapshot measures of plant ecophysiological activity at the time of sampling (e.g. leaf gas exchange; Dawson et al., 2002; Wittmer et al., 2008). Moreover, the stable isotope approach is less time-consuming and labor-demanding and is more practical for research encompassing multiple remote field sites, thereby permitting more ambitious sampling schemes with higher sampling intensity and replication (Querejeta et al., 2022).

Here we investigated the physiological and nutritional responses of *S. tenacissima* to joint changes in aridity and shrub encroachment along a 350 km climatic gradient in the Iberian Peninsula. We used a classic space-for-time substitution approach to asses *S. tenacissima* responses to ongoing aridification, and combined time-integrated information on physiological activity by analysing the natural variations in leaf stable isotopes ($\delta^{18}O$, $\delta^{13}C$, $\delta^{15}N$) and nutrient (N, P, K) concentrations, with measures of plant water status (culm water content [CWC]) and uptake (culm water isotopic composition; $\delta^{18}O$, $\delta^{2}H$). The $\delta^{2}H$ and $\delta^{18}O$ values of grass culm water and its deuterium excess ($d\text{-excess} = \delta^{2}H - 8 \times \delta^{18}O$; Dansgaard, 1964) provide a powerful tool to assess the water sources used by dryland species (Illuminati et al., 2022). We hypothesised that increasing climate aridity will reduce the perennial grass cover of *S. tenacissima* steppes as a result of lower stomatal conductance and more stringent stomatal constraints on carbon assimilation and productivity with increasing drought stress in this drought-avoider species (Konings et al., 2017; Liu et al., 2020; Wittmer et al., 2008). We also hypothesised that woody shrub encroachment will further exacerbate the negative impacts of increasing aridity on the water and nutrient status, productivity and perennial grass cover of *S. tenacissima* steppes through enhanced diffuse competition for limiting soil moisture and nutrients.

2 | MATERIALS AND METHODS

2.1 | Study area and climatic variables evaluated

We selected 10 locations along a ~350 km transect from Central to Southeastern Spain (Figure S1) representing an increasing climatic aridity gradient encompassing much of the geographical distribution of *S. tenacissima* in the Iberian Peninsula, including areas with MAP ranging from 346 to 464 mm and mean annual temperature (MAT) from 12.6 to 16.3°C (Tables S1 and S2). The climate is semiarid Mediterranean, with asynchronous wet and warm seasons, as maximum and minimum precipitation fall in winter and summer, respectively. The soils are classified as Calcisols and are weakly developed and thin, with sandy loam texture and high pH values (>7–8) (Maestre et al., 2009). Transpiration fluxes and primary productivity in semiarid *S. tenacissima* steppes are rather low, with peak plant ecophysiological activity occurring shortly after the irregular rainfall pulses (Domingo et al., 2011).

Using the geographical coordinates of each location, we obtained the elevation and available climatic information from Worldclim (http://www.worldclim.org; Hijmans et al., 2005) and measured the minimum distance to the Mediterranean Sea (DTMS) using Google Earth. Climate variables included temperature and precipitation (mean annual, average of the wettest and coldest quarter and month, average of the driest and warmest quarter and month). We calculated the aridity for each location as $A = 1 - (\text{annual precipitation/annual potential evapotranspiration})$. Mean annual VPD for each location was obtained from TerraClimate data (Abatzoglou et al., 2018). Several geographic and climatic variables showed substantial multi-collinearity along the aridity gradient (Table S3).

2.2 | Field surveys

Field sampling was conducted during May 2008, and no permissions were needed for fieldwork. At each sampling location, we selected two paired sites with contrasting woody shrub cover (i.e. pure *S. tenacissima* grass steppes vs. nearby shrub-encroached steppes with 26.4% shrub cover; see Maestre et al., 2009), totalling 20 sites. The encroaching shrubs species were *Quercus coccifera*, *Pistacia lentiscus*, *Rhamnus lycioides*, *Juniperus phoenicea* and *Juniperus oxycedrus*. Plant cover at each site was measured using the point-intercept methodology in four 30-m transects separated 8 m from each other.

At each of the 20 sites, we sampled eight adult *S. tenacissima* individuals, (replicates) resulting in 160 individuals. The canopy size of each tussock individual was measured using two diameters (parallel and perpendicular to the steepest slope) and calculated using the formula for the area of an ellipse. At sites undergoing woody shrub encroachment, we sampled tussock individuals located at a fixed distance (5-m) from the canopy edge of woody shrubs to exclude direct, immediate competition effects between shrubs and *S. tenacissima* at close range. Our assessment of how woody shrub encroachment impacts on the water and nutrient status of *S. tenacissima* focuses on diffuse competitive effects of encroaching shrubs and therefore excludes the effects of direct, interspecific shrub-grass interactions at close range.

2.3 | Isotopic and nutrient analyses

Fully expanded and healthy-looking leaves with their corresponding basal culms were collected for isotopic and nutrient analyses. Green leaf samples were oven-dried (60°C, 24 h) and finely ground using a ball mill. Leaf $\delta^{13}C$ and $\delta^{15}N$ were measured by continuous flow dual isotopic analysis using an IsoPrime 100 IRMS (IsoPrime, UK) interfaced to a CHNOS C/N Elemental Analyser. Leaf $\delta^{18}O$ was measured in continuous flow using an Elementar PYRO Cube interfaced to a Thermo Finnigan Delta V IRMS (Thermo Finnigan, Germany). The analytical precision was ±0.1‰ for leaf $\delta^{13}C$ and ±0.2‰ for leaf $\delta^{18}O$ and $\delta^{15}N$. Ground leaves were digested with HNO_3:$HClO_4$ (2:1, v:v) and P and K concentrations measured in the digested solution by a Perkin Elmer Inductively Coupled Plasma 5500 atomic absorption spectrometer.

Time-integrated WUEi at leaf level was estimated based on foliar $\delta^{13}C$ values (Cernusak et al., 2013) as determined by the atmospheric CO_2 concentration (385.97 ppm in 2008) and the ratio of atmospheric [CO_2] to intracellular [CO_2] (c_i/c_a) as follows:

$$\mathrm{WUEi} = A / g_s = c_a \left[1 - \left(c_i / c_a\right)\right] \times 0.625, \quad (1)$$

$$\delta^{13}C_{leaf} = \delta^{13}C_{atm} - a - (b - a) \times \left(c_i / c_a\right), \quad (2)$$

where $\delta^{13}C_{leaf}$ is the foliar isotope ratio, $\delta^{13}C_{atm}$ is isotopic ratio of atmospheric CO_2 (−8.321‰ in 2008) and a and b are isotopic fractionation factors associated with CO_2 diffusion (4.4‰) and Rubisco discrimination (27‰), respectively.

Non-transpiring basal culms (5–6) from the base of the perennial tussock grasses near ground level were collected from each target individual as a proxy of the isotopic signature of source water used by *S. tenacissima* at the peak of the growing season. The basal culms were quickly placed in capped glass vials, sealed with parafilm, transported in coolers, and stored in the freezer (−20°C) until water extraction. Water extractions were performed using cryogenic vacuum distillation and lasted 2–4 h at 105°C until culm water was extracted completely. CWC was calculated as:

$$\mathrm{CWC} = \left(W_{wet} - W_{dry}\right) / W_{wet} \cdot 100\,\%, \quad (3)$$

where W_{wet} is the weight of fresh culm sample and W_{dry} is the weight of culm sample after water extraction. The culm water $\delta^{18}O$ and $\delta^{2}H$ values of half of the samples ($n = 80$) were determined by continuous flow using a Thermo Gas Bench II interfaced to a Thermo Finnigan Delta plus XL IRMS (Thermo Finnigan, Germany). The analytical precision was ±0.12‰ for $\delta^{18}O$, and ±0.6‰ for $\delta^{2}H$. Water extracted from non-transpiring tissues in grasses inevitably includes some phloem water mixed with xylem water, which may cause some isotopic fractionation issues (Barnard et al., 2006; Jiang et al., 2022).

2.4 | Statistical analyses

We performed a principal component analysis (PCA) with three water related traits (CWC, leaf $\delta^{13}C$, $\delta^{18}O$) to obtain a multidimensional overview of plant water status. We then extracted the loadings of the first PCA axes (PCA_{Axis1}) and used them as an additional plant variable. To test the relationships between key geographic and climate variables and *S. tenacissima* traits and PCA_{Axis1} scores across individuals ($n = 160$) we used linear mixed regression models with each geographic or climate variable as predictor and plant traits as dependent variable with site included as a random factor. Additionally, we tested relationships between *S. tenacissima* traits using standardised major axis regressions. We analysed the impact of shrub encroachment on *S. tenacissima* traits and PCA_{Axis1} scores using general linear mixed models with *shrub encroachment* as a fixed factor and site included as a random factor. All calculations and statistical analyses were performed with the R software (R Core Team, 2022) using the packages *ade4* (Chessel et al., 2004), *effects* (Fox, 2002), *emmeans* (Lenth, 2020), *Hmisc* (Harell, 2019), *lme4* (Bates et al., 2015) and *smatr* (Warton et al., 2012).

3 | RESULTS

3.1 | Changes in leaf isotopic compositions and nutrient concentrations

Leaf $\delta^{13}C$ ranged from −25.84‰ to −21.11‰ along the aridity gradient (average −23.43 ± 0.07‰, $n = 160$), which translated into very high WUE_i values ranging from 96.3 to 148.8 μmol CO_2 mol^{-1} H_2O (Figure 1a,b). Leaf $\delta^{13}C$ increased with aridity

(slope = 8.962, R^2_{mar} = 0.15, p = 0.041) and VPD (slope = 1.4078, R^2_{mar} = 0.18, p = 0.022), whereas it decreased with distance from the Mediterranean Sea (DTMS; slope = −0.004, R^2_{mar} = 0.22, p = 0.007) and latitude (slope = −0.428, R^2_{mar} = 0.24, p = 0.004) (Table S4). Leaf $\delta^{13}C$ values were thus higher at the drier sites, indicating increasing WUEi with increasing climatic aridity and atmospheric dryness (Figure 1a,b). Average precipitation during the coldest quarter (PCQ) at each location was the best predictor of leaf $\delta^{13}C$ variation across the aridity gradient (slope = −0.031, R^2_{mar} = 0.25, p = 0.003; Table S5; Figure 2a), revealing increasing WUEi with decreasing winter precipitation.

Leaf $\delta^{18}O$ values ranged from 28.31 to 32.48‰ along the aridity gradient (30.49 ± 0.07‰ average, n = 160), and decreased with MAP (slope = −0.013, R^2_{mar} = 0.21, p = 0.049; Table S4) and altitude (slope = −0.004, R^2_{mar} = 0.31, p = 0.010; Table S4). Average precipitation during the warmest quarter (PWAQ) was the best predictor of leaf $\delta^{18}O$ variation (slope = −0.064, R^2_{mar} = 0.36, p = 0.003; Table S5; Figure 2b), indicating higher leaf $\delta^{18}O$ values at sites with drier summers. Higher leaf $\delta^{18}O$ values thus occurred in drier sites located at lower elevation, indicating lower time-integrated stomatal conductance with increasing drought stress. Moreover, a positive association between leaf $\delta^{13}C$ and $\delta^{18}O$ across all the individuals sampled (R^2 = 0.025, p = 0.047, slope = 0.940) further supported a shared stomatal control over both isotopic variables.

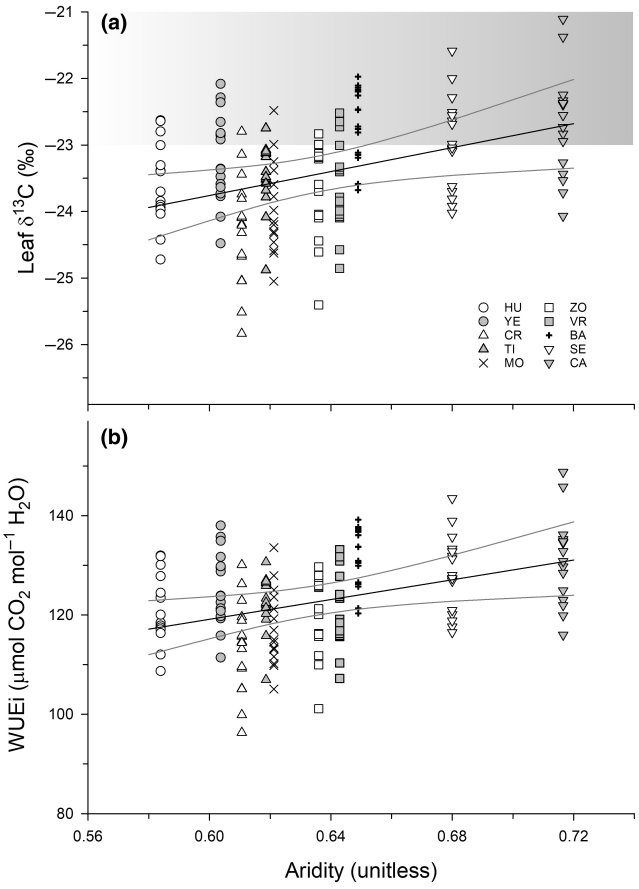

FIGURE 1 Variations of leaf $\delta^{13}C$ (a) and calculated time-integrated Intrinsic water use efficiency (b) values with aridity for *Stipa tenacissima* individuals. The shaded area in the upper panel represents the physiological limit for C_3 photosynthetic metabolism (−23‰ according to Kohn, 2010). Abbreviations for study locations are given in the caption of Figure S1.

Leaf N was not related to any geographic or climatic variables (Tables S4 and S5) and was consistently low along the entire aridity gradient, with values ranging from 0.53% to 1.08% (0.78 ± 0.01% average, n = 160) that suggest severe N limitation of perennial grass photosynthesis and productivity across all the sites. Leaf N:P ratios were remarkably low and ranged between 4.17 and 11.47 across individuals (7.82 ± 0.09 average), which further supports N limitation of *S. tenacissima* productivity in these semiarid steppes. Leaf $\delta^{15}N$ values ranged from −5.39‰ to 0.27‰ (−2.34 ± 0.09‰ average, n = 160) and showed no significant relationship with any climatic or geographic variables (Tables S4 and S5). $\delta^{15}N$ increased with CWC (R^2 = 0.10, p < 0.001, slope = 0.194; Figure 3), leaf P concentration (R^2 = 0.05, p = 0.005, slope = 73.98) and N concentration (R^2 = 0.02, p = 0.081, slope = 10.34). Foliar P was not related to any geographic or climatic variables (Tables S4 and S5), whereas leaf K decreased with increasing average PWAQ (R^2_{mar} = 0.31, p = 0.004, slope = −0.005; Table S5), indicating greater foliar K accumulation at locations with drier summers. Higher foliar K was also linked to higher leaf $\delta^{18}O$ values (R^2 = 0.08, p < 0.001, slope = 7.23; Figure S2) suggesting tighter stomatal regulation of transpiration flux with increasing foliar K accumulation.

3.2 | Changes in CWC and isotopic compositions of *S. tenacissima*

CWC decreased with MAT (slope = −2.385, R^2_{mar} = 0.15, p = 0.018; Table S4) and increased with precipitation during the driest quarter (slope = −0.218, R^2_{mar} = 0.13, p = 0.031; Table S5). Across sites and individuals, lower CWC was linked to higher leaf $\delta^{13}C$ (R^2 = 0.05, p = 0.006, slope = −6.67), $\delta^{18}O$ (R^2 = 0.03, p = 0.031, slope = −6.22) and $\Delta^{18}O$ (R^2 = 0.14, p = 0.001, slope = −6.22) values, overall suggesting lower stomatal conductance and higher leaf-level WUEi with increasing plant drought stress. A PCA analysis of water-related plant traits (leaf $\delta^{13}C$, $\delta^{18}O$, CWC) yielded a single axis of covariation encompassing 46% of the variance with heavy loadings of the three traits (0.600, 0.536, −0.604, respectively). Individual plant scores along this axis increased with increasing climate aridity, indicating higher leaf $\delta^{13}C$ and $\delta^{18}O$ and lower water content at more arid sites (slope = 16.72, R^2_{mar} = 0.26, p = 0.011; Figure 4).

Regarding culm water isotopic composition, both $\delta^{18}O_{cw}$ and $\delta^{2}H_{cw}$ decreased with DTMS (slope = −0.0082, R^2_{mar} = 0.32, p = 0.012 and slope = −0.0792, R^2_{mar} = 0.49, p = 0.008, respectively; Table S4) and latitude (slope = −0.712, R^2_{mar} = 0.24, p = 0.039 and slope = −7.154, R^2_{mar} = 0.40, p = 0.023, respectively; Table S4). This pattern matches the expected natural variation of mean rainwater isotopic composition along the aridity gradient. The slope of the $\delta^{2}H$ versus $\delta^{18}O$ bi-plot obtained from culm water isotopic values was rather similar to the slope of the global meteoric water line (GMWL) representing

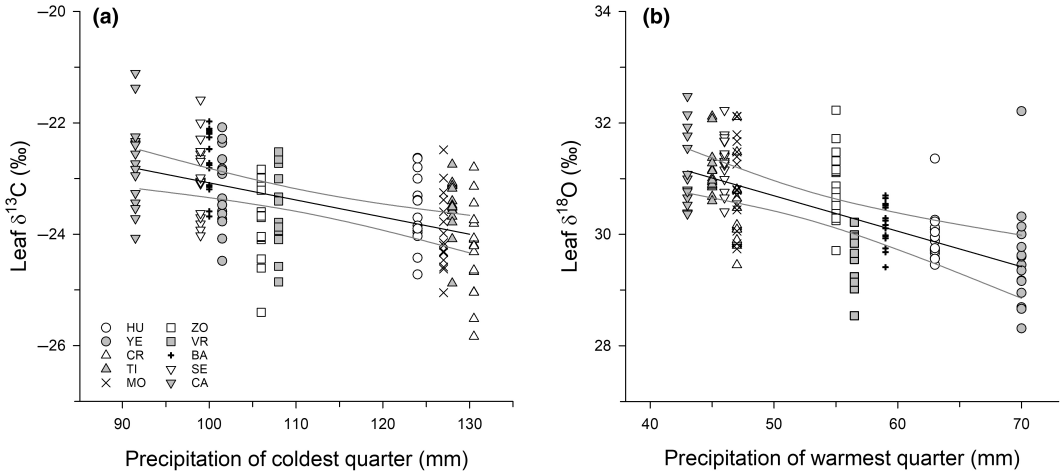

FIGURE 2 Variations of leaf $\delta^{13}C$ with average precipitation during the coldest quarter of the year (a, winter) and leaf $\delta^{18}O$ with average precipitation during the warmest quarter of the year (b, summer) for *Stipa tenacissima* individuals. Abbreviations for study locations are given in the caption of Figure S1.

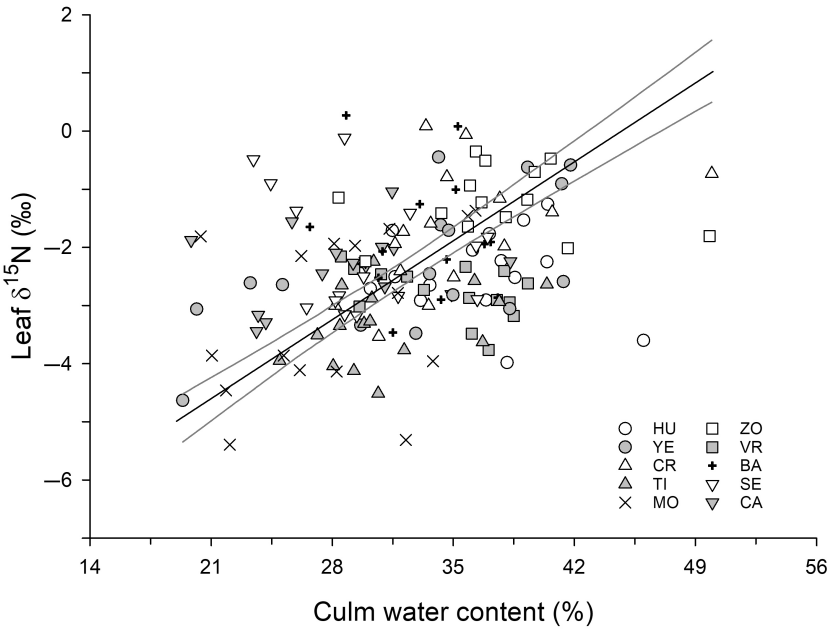

FIGURE 3 Leaf $\delta^{15}N$ plotted against culm water content for *Stipa tenacissima* individuals at 10 sampling locations along the aridity gradient studied. Abbreviations for study locations are given in the caption of Figure S1.

the isotopic composition of rainwater (CWC slope = 7.67 vs. GMWL slope = 8; Figure S3), indicating that any isotopic fractionation issues during root water uptake were rather minor.

Culm water oxygen isotopic composition ($\delta^{18}O_{cw}$) and leaf $\delta^{18}O$ values were unrelated across individuals ($p = 0.38$, $n = 76$), indicating that geographical variation in rainwater isotopic composition was not the primary driver of foliar $\delta^{18}O$ variation. A strong stomatal signal superimposed on the source water isotope signal thus appears to drive the variation in foliar $\delta^{18}O$ along the aridity gradient, which may explain the lack of any significant association between leaf $\delta^{18}O$ and $\delta^{18}O_{cw}$ across all the sampled perennial grass individuals. Leaf oxygen isotope enrichment above source water ($\Delta^{18}O = \delta^{18}O_{leaf} - \delta^{18}O_{cw}$) was positively related to leaf $\delta^{18}O$ ($R^2 = 0.18$, $p < 0.001$, slope = 0.512), but was unrelated to $\delta^{13}C$ ($p = 0.93$), MAT, MAP or aridity (Table S4, $n = 76$).

3.3 | Changes in plant cover along the aridity gradient

Plant cover ranged from 36.2% to 67.8% (average 51.5 ± 0.77%), decreased with MAT (slope = −6.005, $R^2_{mar} = 0.30$, $p = 0.050$) but increased with MAP (slope = 0.161, $R^2_{mar} = 0.26$, $p = 0.068$), latitude (slope = 7.194, $R^2_{mar} = 0.47$, $p = 0.008$) and DTMS (slope = 0.0767, $R^2_{mar} = 0.54$, $p = 0.003$, Table S4). Total plant cover and perennial grass cover were both strongly responsive to variation in precipitation during winter (PCQ) along the aridity gradient. Both of them decreased steeply with declining PCQ (slope = 0.540, $R^2_{mar} = 0.47$, $p = 0.003$ and slope = 0.591, $R^2_{mar} = 0.30$, $p = 0.037$, respectively; Table S5), thereby reflecting a declining density of perennial tussock grass individuals per unit area with increasing

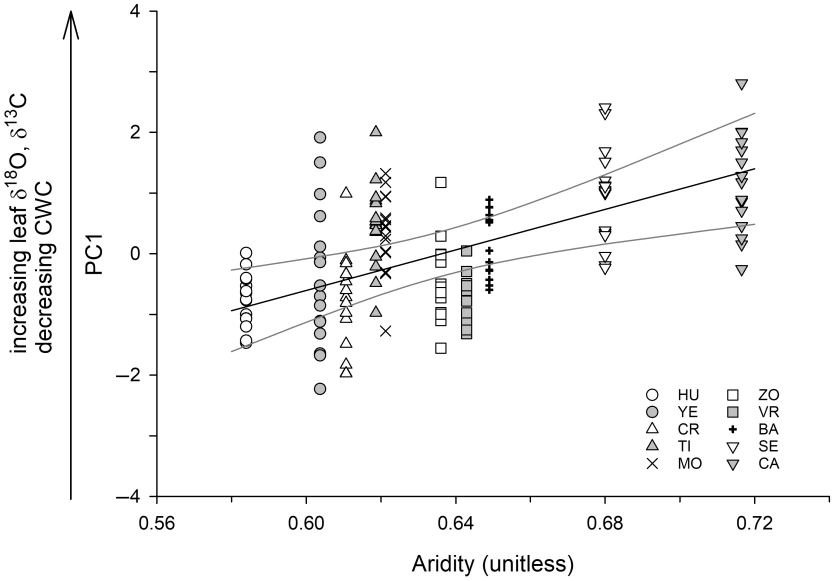

FIGURE 4 Variation of the PCA_{Axis1} scores derived from three water-related plant traits (culm water content [CWC], leaf $\delta^{18}O$ and $\delta^{13}C$) with aridity for *Stipa tenacissima* individuals at 10 sampling locations along the studied aridity gradient. The black arrow beside the left axis represents the continuum of increasing leaf $\delta^{18}O$ and $\delta^{13}C$ values with decreasing CWC. Abbreviations for study locations are given in the caption of Figure S1.

TABLE 1 Mean values and results from general linear mixed models for shrub encroachment impact on *S. tenacissima* traits and the first axis of the principal component analysis (PC1) along the aridity gradient studied.

Trait	Pure grass steppe	Shrub-encroached steppe	*F*-value	*p*-Value
Plant cover (%)	51.8 ± 1.1	51.2 ± 1.1	0.738	0.392
Tussock size (cm^2)	3835 ± 223	4147 ± 271	1.058	0.305
Perennial grass cover (%)	44.7 ± 1.7	32.6 ± 1.1	**227.36**	**<0.001**
Culm water content (%)	32.4 ± 0.7	33.1 ± 0.6	0.643	0.424
Culm water $\delta^{18}O$ (‰)	−6.37 ± 0.24	−6.27 ± 0.20	0.203	0.654
Culm water $\delta^{2}H$ (‰)	−47.52 ± 1.75	−47.74 ± 1.67	0.052	0.821
$\delta^{18}O_{leaf}$ (‰)	30.58 ± 0.11	30.41 ± 0.09	3.115	0.080
$\Delta^{18}O_{leaf}$ (‰)	36.89 ± 0.27	36.64 ± 0.21	1.143	0.289
$\delta^{13}C_{leaf}$ (‰)	−23.43 ± 0.10	−23.44 ± 0.09	0.008	0.930
$\delta^{15}N_{leaf}$ (‰)	−2.43 ± 0.14	−2.25 ± 0.10	1.549	0.215
Leaf N (%)	0.783 ± 0.012	0.779 ± 0.011	0.102	0.750
Leaf P (%)	0.105 ± 0.002	0.097 ± 0.001	**16.160**	**<0.001**
Leaf K (%)	0.636 ± 0.014	0.597 ± 0.013	**8.128**	**0.005**
PC1 (unitless)	0.08 ± 0.12	−0.08 ± 0.11	1.494	0.224

Note: Shown are the site-averaged values (mean ± SE), *F* and *p* values (significant relationships, i.e. $p < 0.05$, are in bold).

water limitation of photosynthesis and productivity along the aridity gradient.

3.4 | Impacts of shrub encroachment on *S. tenacissima* leaf traits and cover

Shrub encroachment in semiarid steppes significantly reduced the leaf P and K concentrations of *S. tenacissima* (Table 1), indicating enhanced diffuse competition for these limiting nutrients between perennial grasses and encroaching shrubs, even though close-range (<5 m) competitive effects were excluded. However, contrary to expectations, there were no significant impacts of shrub encroachment on the average size of individual *S. tenacissima* tussocks or their leaf N concentration, foliar $\delta^{18}O$, $\delta^{13}C$, $\delta^{15}N$, CWC or $\delta^{18}O/\delta^{2}H$. Nonetheless, *S. tenacissima* cover decreased significantly with shrub encroachment, from an average of 44.7 ± 3.4% in pure grass steppes to an average of 32.6 ± 3.1% in shrub-encroached steppes ($p < 0.001$).

4 | DISCUSSION

Higher foliar $\delta^{13}C$ values toward the hotter and drier end of the climatic gradient in *S. tenacissima* suggest that perennial grasses may experience adequate soil moisture conditions less frequently with increasing aridity, and may thus be forced to extend their physiological activity and carbon gain further into drought periods with suboptimal water availability. Higher $\delta^{13}C$ with increasing aridity thus revealed that improved WUEi at the drier and hotter end of

the gradient is primarily (if not exclusively) achieved through more stringent stomatal regulation of transpiration and photosynthesis, and therefore at the likely cost of lower carbon assimilation and productivity.

4.1 | Increases in climatic aridity negatively impact the water status of *S. tenacissima*

Leaf $\delta^{13}C$ and $\delta^{18}O$ indicate that time-integrated stomatal constraints on photosynthesis increase markedly with climatic dryness, thereby forcing perennial grasses to operate at enhanced WUEi. *S. tenacissima* reaches exceptionally high leaf $\delta^{13}C$ values in our semiarid steppes, ranging from −25.84‰ to −21.11‰ across individuals (12.64‰ to 18.1‰ in $\Delta^{13}C$ scale). Previous studies reported similarly high leaf $\delta^{13}C$ values in semiarid *S. tenacissima* steppes of the Iberian Peninsula (Maestre & Cortina, 2006; Ramírez et al., 2009). The leaf $\delta^{13}C$ and WUEi values of *S. tenacissima* are among the highest in the literature for dryland or desert C_3 plants (Cornwell et al., 2018; Diefendorf et al., 2010; Hartman & Danin, 2010; Querejeta et al., 2022; Wang et al., 2016), often reaching or even surpassing the theoretical physiological limits for C_3 photosynthetic metabolism in angiosperms (−23‰ threshold; Kohn, 2010). Site-averaged leaf $\delta^{13}C$ values at our most arid sites (ranging from -22.97 ± 0.18 to -22.67 ± 0.14‰) were even higher than the above-mentioned threshold (Figure 1a). The average leaf $\delta^{13}C$ value across all sites was also very close to this theoretical physiological limit (-23.43 ± 0.07‰, $n = 160$). *S. tenacissima* can thus achieve exceptionally stringent stomatal regulation of transpiration and can operate at extremely low internal c_i/c_a ratios in response to severe water limitation. As a reference, the estimated time-integrated WUEi values of *S. tenacissima* in our study (96.3–148.8 μmol CO_2 mol^{-1} H_2O) are even higher than those of native desert shrub species from the US Southwest (80–124.5 μmol CO_2 mol^{-1} H_2O; Kannenberg et al., 2021). Our experimental design cannot distinguish the extent to which the observed increase in WUEi along the aridity gradient is driven by intraspecific genetic differences among distinct *S. tenacissima* populations (local adaptation), phenotypic physiological plasticity or both (Krichen et al., 2022).

The extremely high leaf $\delta^{13}C$ and WUE_i values of *S. tenacissima* are even more remarkable when considering its rather low foliar N concentrations across sites, given the universal scaling of carboxylation and photosynthetic capacity with leaf N (Wright et al., 2004). Therefore, the high $\delta^{13}C/WUE_i$ values of *S. tenacissima* must be primarily achieved by exceptionally stringent stomatal regulation, rather than by a high carboxylation and photosynthetic capacity (Kannenberg et al., 2021). Low leaf N may thus compromise the capacity of *S. tenacissima* steppes to maintain productivity and cope with ongoing climate change at the warmest and driest sites along the aridity gradient. Anthropogenic N deposition coupled with rising atmosphere CO_2 could in theory allow additional increases in WUEi through enhanced leaf N and carboxylation capacity, and/or even more stringent stomatal regulation of plant water flux with the atmospheric CO_2 fertilisation effect (Donohue et al., 2012). Alternatively, *S. tenacissima* might simply use any additional N to produce more tillers, without any further improvements in WUEi. However, whether the combination of anthropogenic N deposition with the CO_2 fertilisation effect could compensate the negative physiological impacts of forecasted increases in climatic aridity (Trenberth et al., 2014) remains a subject for future research.

The remarkably low N:P ratios of *S. tenacissima* further support nitrogen limitation of photosynthesis (Güsewell, 2004; Tian et al., 2018). Co-occurring native shrubs inhabiting the same semiarid steppes exhibit considerably higher leaf N concentrations, N:P ratios and photosynthetic rates combined with lower $\delta^{13}C$ and $\delta^{18}O$ values than *S. tenacissima* (León-Sánchez et al., 2018, 2020; Moreno-Gutiérrez et al., 2012, 2015; Prieto & Querejeta, 2020). The combination of very low leaf nutrient contents and very high foliar $\delta^{13}C$ and $\delta^{18}O$ values in *S. tenacissima* indicates an exceptionally conservative resource use strategy along the "fast-slow" plant economic spectrum (Prieto et al., 2018; Reich, 2014; Wright et al., 2004). This suggests that the productivity of *S. tenacissima* steppes may be particularly vulnerable to any future climate change-induced increases in aridity that further exacerbate the already stringent stomatal and N constraints on photosynthesis found under the current climate. The declining cover of *S. tenacissima* with increasing aridity and decreasing winter rainfall further supports lower photosynthesis and productivity under warmer and drier climatic conditions in Iberian semiarid steppes, as observed elsewhere (Ghiloufi et al., 2016).

Leaf $\delta^{15}N$ correlated with CWC (proxy of microsite water availability), thereby highlighting the tight coupling and interplay between soil water availability and N cycling dynamics in dryland ecosystems (Bai et al., 2009; Handley et al., 1999; Wang et al., 2014). In drylands, biogeochemical N cycling rates tend to increase with soil moisture that favours microbial activity and gaseous ^{15}N-depleted nitrogen loss, eventually leading to greater ^{15}N enrichment in the remaining soil N pools. This may explain why *S. tenacissima* individuals growing in moister microsites (as inferred from higher CWC) show higher leaf $\delta^{15}N$ values in semiarid steppes (Driscoll et al., 2021). Leaf $\delta^{15}N$ also increased with leaf P and N, overall indicating that *S. tenacissima* individuals growing in moister and more nutrient-rich microsites may benefit from locally faster N biogeochemical cycling rates (Ruiz-Navarro et al., 2016).

Culm water isotopes ($\delta^{18}O$ and $\delta^{2}H$) revealed that *S. tenacissima* primarily uses recent rainwater exposed to negligible evaporative fractionation and isotopic enrichment prior to root uptake. Moreover, the site-averaged *d*-excess of culm water showed a very narrow range of values from 8.5‰ to −4.8‰, which further indicates that *S. tenacissima* consistently uses recent, fresh rainwater with little or no evidence of evaporative isotope enrichment (Dansgaard, 1964; Dawson et al., 2002). *S. tenacissima* appears to be heavily dependent on the rapid root uptake of fresh rainwater present in topsoil shortly after rainfall pulses, when topsoil water still conserves the original isotopic signature of rainwater, before any significant evaporative isotopic fractionation can take place.

This heavy dependence on recent rainwater suggests limited potential for shifting to deeper, wetter soil layers for water uptake during prolonged rainless spells. Its shallow water uptake pattern may force *S. tenacissima* to close stomata early and thus drastically reduce or suppress photosynthetic activity when topsoil water content is depleted during drought periods. This could render *S. tenacissima* vulnerable to the longer and more frequent rainless periods combined with faster warming-induced topsoil drying expected with ongoing climate aridification, which might contribute to further impair the nutrient status and reduce the productivity of these semiarid steppes in future decades (Querejeta, Ren, et al., 2021).

A positive link between leaf K concentration and $\delta^{18}O$ across individuals revealed the coupling of higher foliar K accumulation with reduced time-integrated stomatal conductance in *S. tenacissima* under increasing aridity and drought stress. Enhanced root K uptake and accumulation in leaves can improve plant internal osmotic adjustment, stomatal regulation and guard-cell closure of stomatal pores, thereby reducing stomatal conductance and favouring water savings under heat and drought stress in dryland species (Rivas-Ubach et al., 2012; Sardans & Peñuelas, 2015). Interestingly, both leaf $\delta^{18}O$ and K concentration were best predicted by average precipitation of the warmest quarter (Table S5). This suggests that enhanced foliar K accumulation and subsequent K-induced improvements in osmoregulation and fine-tuned stomatal regulation of plant water flux may be required to foster plant drought endurance during the stressful Mediterranean summers at the most arid end of the climate gradient (Benlloch-González et al., 2008).

4.2 | Shrub encroachment decreases the leaf P and K concentrations of *S. tenacissima*

Lower foliar P and K with shrub encroachment reveals diffuse interspecific competition for these nutrients by shrubs (Craine & Dybzinski, 2013), even when excluding direct plant–plant competitive effects at close range (<5 m). This finding is consistent with the notion that shrub encroachment often reduces the nutritional quality of grasses for herbivores in drylands (Zarovali et al., 2007). We found no evidence of any negative impacts of woody shrub encroachment on the water status of *S. tenacissima* through diffuse competition for soil moisture in these semiarid steppes, at least when short-range (<5 m) competitive interactions are excluded. The dissimilar root system sizes and depths between coexisting grasses and woody shrubs favour ecohydrological niche segregation and water source partitioning between them, thereby reducing diffuse competition for topsoil moisture (Illuminati et al., 2022; Moreno-Gutiérrez et al., 2012, 2015). However, *S. tenacissima* cover still decreased significantly with shrub encroachment, thereby indicating that the overall impact of shrub encroachment on perennial grasses (which also includes direct plant–plant interactions at close range that were not considered in our study) was by no means entirely neutral (Eldridge et al., 2011).

In conclusion, *S. tenacissima* will likely respond to the ongoing climate warming and drying trend with tighter stomatal regulation of plant water fluxes and reduced stomatal conductance to adaptively enhance leaf-level WUEi, which will further increase the already severe stomatal constraints on carbon assimilation and productivity (Liu et al., 2020). This interpretation is supported by the significant trends toward lower perennial tussock grass cover in semiarid steppes with increasing aridity. Our findings thus highlight the physiological limits and constraints of the drought-avoidance strategy based on early stomatal closure during rainless periods to cope with climate aridification in shallow-rooted dryland species. They also indicate that any further adaptive plastic increase in WUEi through further reductions in stomatal conductance is unlikely to offset the detrimental impacts of aridification on the photosynthesis, productivity and cover of *S. tenacissima*, especially at the drier parts of their current distribution.

AUTHOR CONTRIBUTIONS

José Ignacio Querejeta and Fernando T. Maestre conceived the research and obtained funding. Santiago Soliveres and Pablo García-Palacios conducted all field sampling and measurements. Wei Ren performed laboratory work and wrote the first draft. José Ignacio Querejeta, Iván Prieto and Wei Ren analysed and interpreted the data. José Ignacio Querejeta wrote the final version, with contributions from all co-authors.

ACKNOWLEDGEMENTS

This research was funded and supported by grants from the Spanish Ministry of Science and Innovation (AGL-2006-11234; CGL2010-21064; CGL2013-48753-R; PID2019-107382RB-I00; PRX19/00301) awarded to JIQ, and grants by Fundación BBVA (BIOCON06/105) and Universidad Rey Juan Carlos (URJC-RNT-063-2) awarded to FTM. FTM also acknowledges support from the European Research Council (ERC Grant agreement 647038 [BIODESERT]), Generalitat Valenciana (CIDEGENT/2018/041) and the Spanish Ministry of Science and Innovation (EUR2022-134048). WR acknowledges partial support from the National Natural Science Foundation of China (41801091) and China Postdoctoral Science Foundation (2019T120868 and 2018M643542). SS was supported by a Ramón y Cajal fellowship (RYC-2016-20604) and the FOBIASS project (RTI2018-098895-A-100), both from the Spanish Ministry of Science and Innovation. PGP was supported by the DUALSOM project (PID2020-113021RA-I00) from the Spanish Ministry of Science and Innovation. IP was supported by the Fundación Séneca (project 20654/JLI/18). The authors thank María José Espinosa for help with laboratory work.

CONFLICT OF INTEREST STATEMENT

The authors have declared no conflicts of interest. Pablo García-Palacios is an Associate Editor of Functional Ecology but took no part in the peer review and decision-making processes for this paper.

DATA AVAILABILITY STATEMENT

All data are present in the manuscript or Supporting Information. Data can be publicly accessed via the following link: https://doi.org/10.5061/dryad.pzgmsbcv4.

ORCID

Santiago Soliveres https://orcid.org/0000-0001-9661-7192
Iván Prieto https://orcid.org/0000-0001-5549-1132
José Ignacio Querejeta https://orcid.org/0000-0002-9547-0974

REFERENCES

Abatzoglou, J. T., Dobrowski, S. Z., Parks, S. A., & Hegewisch, K. C. (2018). TerraClimate, a high-resolution global dataset of monthly climate and climatic water balance from 1958–2015. *Scientific Data*, *5*, 170191.

Alguacil, M.d. M., Schlaeppi, K., López-García, Á., Heijden, M. G. A.v.d., & Querejeta, J. I. (2022). Contrasting responses of arbuscular mycorrhizal fungal families to simulated climate warming and drying in a semiarid shrubland. *Microbial Ecology*, *84*, 941–944.

Bai, E., Boutton, T. W., Liu, F., Wu, X. B., Archer, S. R., & Hallmark, C. T. (2009). Spatial variation of the stable nitrogen isotope ratio of woody plants along a topoedaphic gradient in a subtropical savanna. *Oecologia*, *159*, 493–503.

Balaguer, L., Pugnaire, F., Martínez-Ferri, E., Armas, C., Valladares, F., & Manrique, E. (2002). Ecophysiological significance of chlorophyll loss and reduced photochemical efficiency under extreme aridity in *Stipa tenacissima* L. *Plant and Soil*, *240*, 343–352.

Barbour, M. M. (2007). Stable oxygen isotope composition of plant tissue: A review. *Functional Plant Biology*, *34*, 83–94.

Barnard, R. L., de Bello, F., Gilgen, A. K., & Buchmann, N. (2006). The $\delta^{18}O$ of root crown water best reflects source water $\delta^{18}O$ in different types of herbaceous species. *Rapid Communications in Mass Spectrometry*, *20*, 3799–3802.

Bates, D., Mächler, M., Bolker, B., & Walker, S. (2015). Fitting linear mixed-effects models using lme4. *Journal of Statistical Software*, *67*, 1–48.

Benlloch-González, M., Arquero, O., Fournier, J. M., Barranco, D., & Benlloch, M. (2008). K^+ starvation inhibits water-stress-induced stomatal closure. *Journal of Plant Physiology*, *165*, 623–630.

Cernusak, L. A., Ubierna, N., Winter, K., Holtum, J. A. M., Marshall, J. D., & Farquhar, G. D. (2013). Environmental and physiological determinants of carbon isotope discrimination in terrestrial plants. *New Phytologist*, *200*, 950–965.

Chessel, D., Dufour, A.-B., & Thioulouse, J. (2004). The ade4 package—I: One-table methods. *R News*, *4*, 5–10.

Cornwell, W. K., Wright, I. J., Turner, J., Maire, V., Barbour, M. M., Cernusak, L. A., Dawson, T., Ellsworth, D., Farquhar, G. D., Griffiths, H., Keitel, C., Knohl, A., Reich, P. B., Williams, D. G., Bhaskar, R., Cornelissen, J. H. C., Richards, A., Schmidt, S., Valladares, F., … Santiago, L. S. (2018). Climate and soils together regulate photosynthetic carbon isotope discrimination within C_3 plants worldwide. *Global Ecology and Biogeography*, *27*, 1056–1067.

Craine, J. M., & Dybzinski, R. (2013). Mechanisms of plant competition for nutrients, water and light. *Functional Ecology*, *27*, 833–840.

Cramer, M. D., Hawkins, H.-J., & Verboom, G. A. (2009). The importance of nutritional regulation of plant water flux. *Oecologia*, *161*, 15–24.

Dansgaard, W. (1964). Stable isotopes in precipitation. *Tellus A*, *16*, 436–468.

Dawson, T. E., Mambelli, S., Plamboeck, A. H., Templer, P. H., & Tu, K. P. (2002). Stable isotopes in plant ecology. *Annual Review of Ecology and Systematics*, *33*, 507–559.

Diefendorf, A. F., Mueller, K. E., Wing, S. L., Koch, P. L., & Freeman, K. H. (2010). Global patterns in leaf ^{13}C discrimination and implications for studies of past and future climate. *Proceedings of the National Academy of Sciences of the United States of America*, *107*, 5738–5743.

Domingo, F., Serrano-Ortiz, P., Were, A., Villagarcía, L., Garcíad, M., Ramírez, D. A., Kowalski, A. S., Moro, M. J., Reya, A., & Oyonarte, C. (2011). Carbon and water exchange in semiarid ecosystems in SE Spain. *Journal of Arid Environments*, *75*, 1271–1281.

Donohue, R. J., Roderick, M. L., McVicar, T. R., & Farquhar, G. D. (2012). Impact of CO_2 fertilization on maximum foliage cover across the globe's warm, arid environments. *Geophysical Research Letters*, *40*, 3031–3035.

Driscoll, A. W., Kannenberg, S. A., & Ehleringer, J. R. (2021). Long-term nitrogen isotope dynamics in *Encelia farinosa* reflect plant demographics and climate. *New Phytologist*, *232*, 1226–1237.

Eldridge, D. J., Bowker, M. A., Maestre, F. T., Roger, E., Reynolds, J. F., & Whitford, W. G. (2011). Impacts of shrub encroachment on ecosystem structure and functioning: Towards a global synthesis. *Ecology Letters*, *14*, 709–722.

Fox, J. (2002). *An R and S-Plus companion to applied regression*. Sage.

Ghiloufi, W., Quero, J. L., García-Gómez, M., & Chaieb, M. (2016). Potential impacts of aridity on structural and functional status of a southern Mediterranean *Stipa tenacissima* steppe. *South African Journal of Botany*, *103*, 170–180.

Giorgi, F., & Lionello, P. (2008). Climate change projections for the Mediterranean region. *Global and Planetary Change*, *63*, 90–104.

Grossiord, C., Sevanto, S., Bonal, D., Borrego, I., Dawson, T. E., Ryan, M., Wang, W., & McDowell, N. G. (2018). Prolonged warming and drought modify belowground interactions for water among coexisting plants. *Tree Physiology*, *39*, 55–63.

Guiot, J., & Cramer, W. (2016). Climate change: The 2015 Paris Agreement thresholds and Mediterranean basin ecosystems. *Science*, *354*, 465–468.

Güsewell, S. (2004). N:P ratios in terrestrial plants: Variation and functional significance. *New Phytologist*, *164*, 243–266.

Haase, P., Pugnaire, F. I., Clark, S., & Incoll, L. (1999). Environmental control of canopy dynamics and photosynthetic rate in the evergreen tussock grass *Stipa tenacissima*. *Plant Ecology*, *145*, 327–339.

Handley, L., Austin, A., Stewart, G., Robinson, D., Scrimgeour, C., Raven, J., & Schmidt, S. (1999). The ^{15}N natural abundance ($\delta^{15}N$) of ecosystem samples reflects measures of water availability. *Australian Journal of Plant Physiology*, *26*, 185–199.

Harell Jr., F. E. (2019) *Hmisc: Harrell Miscellaneous*. R package Version 3.17-2. Retrieved from: https://CRAN.R-project.org/package=Hmisc

Hartman, G., & Danin, A. (2010). Isotopic values of plants in relation to water availability in the Eastern Mediterranean region. *Oecologia*, *162*, 837–852.

Hijmans, R. J., Cameron, S. E., Parra, J. L., Jones, P. G., & Jarvis, A. (2005). Very high resolution interpolated climate surfaces for global land areas. *International Journal of Climatology*, *25*, 1965–1978.

Illuminati, A., Querejeta, J. I., Pías, B., Escudero, A., & Matesanz, S. (2022). Coordination between water uptake depth and the leaf economic spectrum in a Mediterranean shrubland. *Journal of Ecology*, *110*, 1844–1856.

Jiang, H., Gu, H., Chen, H., Sun, H., Zhang, X., & Liu, X. (2022). Comparative cryogenic extraction rehydration experiments reveal isotope fractionation during root water uptake in Gramineae. *New Phytologist*, *236*, 1267–1280.

Kannenberg, S. A., Driscoll, A. W., Szejner, P., & Ehleringer, J. R. (2021). Rapid increases in shrubland and forest intrinsic water-use efficiency during an ongoing megadrought. *Proceedings of the National Academy of Sciences*, *118*, e2118052118.

Khasanova, A., James, J. J., & Drenovsky, R. E. (2013). Impacts of drought on plant water relations and nitrogen nutrition in dryland perennial grasses. *Plant and Soil*, *372*, 541–552.

Kohn, M. J. (2010). Carbon isotope compositions of terrestrial C_3 plants as indicators of (paleo)ecology and (paleo)climate. *Proceedings of the National Academy of Sciences*, *107*, 19691–19695.

Konings, A. G., Williams, A. P., & Gentine, P. (2017). Sensitivity of grassland productivity to aridity controlled by stomatal and xylem regulation. *Nature Geoscience*, *10*, 284–288.

Krichen, K., Vilagrosa, A., & Chaieb, M. (2022). Morphological and ecophysiological responsiveness of *Stipa tenacissima* L. populations along a Mediterranean climatic gradient. *South African Journal of Botany*, *151*, 116–125.

Le Houérou, H. N. (2001). Biogeography of the arid steppeland north of the Sahara. *Journal of Arid Environments*, *48*, 103–128.

Lenth, R., Buerkner, P., Herve, M., Love, J., Miguez, F., Riebl, H., Singmann, H. (2020) *Emmeans: estimated marginal means, aka least-squares means*. R package Version 1.7.2. https://CRAN.R-project.org/package=emmeans

León-Sánchez, L., Nicolás, E., Goberna, M., Prieto, I., Maestre, F. T., & Querejeta, J. I. (2018). Poor plant performance under simulated climate change is linked to mycorrhizal responses in a semi-arid shrubland. *Journal of Ecology*, *106*, 960–976.

León-Sánchez, L., Nicolás, E., Prieto, I., Nortes, P., Maestre, F. T., & Querejeta, J. I. (2020). Altered leaf elemental composition with climate change is linked to reductions in photosynthesis, growth and survival in a semi-arid shrubland. *Journal of Ecology*, *108*, 47–60.

Levitt, J. (1980). *Responses of plants to environmental stresses. Vol. II. Water, radiation, salt, and other stresses*. Academic Press.

Liu, L., Gudmundsson, L., Hauser, M., Qin, D., Li, S., & Seneviratne, S. I. (2020). Soil moisture dominates dryness stress on ecosystem production globally. *Nature Communications*, *11*, 4892.

Maestre, F. T., Bowker, M. A., Puche, M. D., Hinojosa, M. B., Martínez, I., García-Palacios, P., Castillo, A. P., Soliveres, S., Luzuriaga, A. L., Sánchez, A. M., Carreira, J. A., Gallardo, A., & Escudero, A. (2009). Shrub encroachment can reverse desertification in semi-arid Mediterranean grasslands. *Ecology Letters*, *12*, 930–941.

Maestre, F. T., & Cortina, J. (2006). Ecosystem structure and soil-surface conditions drive the variability in the foliar $\delta^{13}C$ and $\delta^{15}N$ of *Stipa tenacissima* in semiarid Mediterranean steppes. *Ecological Research*, *21*, 44–53.

Mariem, H. B., & Chaieb, M. (2017). Climate change impacts on the distribution of *Stipa tenacissima* L. Ecosystems in North African arid zone—A case study in Tunisia. *Applied Ecology and Environmental Research*, *15*, 67–82.

Martínez-Ferri, E., Balaguer, L., Valladares, F., Chico, J. M., & Manrique, E. (2000). Energy dissipation in drought-avoiding and drought-tolerant tree species at midday during the Mediterranean summer. *Tree Physiology*, *20*, 131–138.

Moreno-Gutiérrez, C., Battipaglia, G., Cherubini, P., Huertas, A. D., & Querejeta, J. I. (2015). Pine afforestation decreases the long-term performance of understorey shrubs in a semi-arid Mediterranean ecosystem: A stable isotope approach. *Functional Ecology*, *29*, 15–25.

Moreno-Gutiérrez, C., Dawson, T. E., Nicolás, E., & Querejeta, J. I. (2012). Isotopes reveal contrasting water use strategies among coexisting plant species in a Mediterranean ecosystem. *New Phytologist*, *196*, 489–496.

Peguero-Pina, J. J., Vilagrosa, A., Alonso-Forn, D., Ferrio, J. P., Sancho-Knapik, D., & Gil-Pelegrín, E. (2020). Living in drylands: Functional adaptations of trees and shrubs to cope with high temperatures and water scarcity. *Forests*, *11*, 1028.

Pivovaroff, A. L., Pasquini, S. C., Guzman, M. E. D., Alstad, K. P., Stemke, J. S., Santiago, L. S., & Field, K. (2016). Multiple strategies for drought survival among woody plant species. *Functional Ecology*, *30*, 517–526.

Prentice, I. C., Meng, T., Wang, H., Harrison, S. P., Ni, J., & Wang, G. (2011). Evidence of a universal scaling relationship for leaf CO_2 drawdown along an aridity gradient. *New Phytologist*, *190*, 169–180.

Prieto, I., & Querejeta, J. I. (2020). Simulated climate change decreases nutrient resorption from senescing leaves. *Global Change Biology*, *26*, 1795–1807.

Prieto, I., Querejeta, J. I., Segrestin, J., Volaire, F., & Roumet, C. (2018). Leaf carbon and oxygen isotopes are coordinated with the leaf economics spectrum in Mediterranean rangeland species. *Functional Ecology*, *32*, 612–625.

Pugnaire, F. I., & Haase, P. (1996). Comparative physiology and growth of two perennial tussock grass species in a semi-arid environment. *Annals of Botany*, *77*, 81–86.

Pugnaire, F. I., Haase, P., Incoll, L. D., & Clark, S. C. (1996). Response of the tussock grass *Stipa tenacissima* to watering in a semi-arid environment. *Functional Ecology*, *10*, 265–274.

Querejeta, J. I., Allen, M. F., Alguacil, M. M., & Roldán, A. (2007). Plant isotopic composition provides insight into mechanisms underlying growth stimulation by AM fungi in a semiarid environment. *Functional Plant Biology*, *34*, 683–691.

Querejeta, J. I., Prieto, I., Armas, C., Casanoves, F., Diémé, J. S., Diouf, M., Yossi, H., Kaya, B., Pugnaire, F. I., & Rusch, G. M. (2022). Higher leaf nitrogen content is linked to tighter stomatal regulation of transpiration and more efficient water use across dryland trees. *New Phytologist*, *235*, 1351–1364.

Querejeta, J. I., Ren, W., & Prieto, I. (2021). Vertical decoupling of soil nutrients and water under climate warming reduces plant cumulative nutrient uptake, water-use efficiency and productivity. *New Phytologist*, *230*, 1378–1393.

Querejeta, J. I., Schlaeppi, K., López-García, Á., Ondoño, S., Prieto, I., Heijden, M. G. A., & Alguacil, M. M. (2021). Lower relative abundance of ectomycorrhizal fungi under a warmer and drier climate is linked to enhanced soil organic matter decomposition. *New Phytologist*, *232*, 1399–1413.

R Core Team. (2022). *R: A language and environment for statistical computing*. R Foundation for Statistical Computing.

Ramírez, D. A., Querejeta, J. I., & Bellot, J. (2009). Bulk leaf $\delta^{18}O$ and $\delta^{13}C$ reflect the intensity of intraspecific competition for water in a semi-arid tussock grassland. *Plant, Cell & Environment*, *32*, 1346–1356.

Ramírez, D. A., Valladares, F., Blasco, A., & Bellot, J. (2008). Effects of tussock size and soil water content on whole plant gas exchange in *Stipa tenacissima* L.: Extrapolating from the leaf versus modelling crown architecture. *Environmental and Experimental Botany*, *62*, 376–388.

Reich, P. B. (2014). The world-wide "fast-slow" plant economics spectrum. *Journal of Ecology*, *102*, 275–301.

Rivas-Ubach, A., Sardans, J., Pérez-Trujillo, M., Estiarte, M., & Peñuelas, J. (2012). Strong relationship between elemental stoichiometry and metabolome in plants. *Proceedings of the National Academy of Sciences of the United States of America*, *109*, 4181–4186.

Ruiz-Navarro, A., Barberá, G. G., Albaladejo, J., & Querejeta, J. I. (2016). Plant $\delta^{15}N$ reflects the high landscape-scale heterogeneity of soil fertility and vegetation productivity in a Mediterranean semiarid ecosystem. *New Phytologist*, *212*, 1030–1043.

Sánchez-Martín, R., Querejeta, J. I., Voltas, J., Ferrio, J. P., Prieto, I., Verdú, M., & Montesinos-Navarro, A. (2021). Plant's gypsum affinity shapes responses to specific edaphic constraints without limiting responses to other general constraints. *Plant and Soil*, *462*, 297–309.

Sardans, J., & Peñuelas, J. (2015). Potassium: A neglected nutrient in global change. *Global Ecology and Biogeography*, *24*, 261–275.

Scheidegger, Y., Saurer, M., Bahn, M., & Siegwolf, R. (2000). Linking stable oxygen and carbon isotopes with stomatal conductance and photosynthetic capacity: A conceptual model. *Oecologia*, *125*, 350–357.

Stewart, G. R., Turnbull, M. H., Schmidt, S., & Erskine, P. D. (1995). ^{13}C natural abundance in plant communities along a rainfall gradient: A biological integrator of water availability. *Functional Plant Biology*, *22*, 51–55.

Tian, D., Yan, Z., Niklas, K. J., Han, W., Kattge, J., Reich, P. B., Luo, Y., Chen, Y., Tang, Z., Hu, H., Wright, I. J., Schmid, B., & Fang, J. (2018). Global leaf nitrogen and phosphorus stoichiometry and their scaling exponent. *National Science Review*, *15*, 728–739.

Trenberth, K. E., Dai, A., Schrier, G.v.d., Jones, P. D., Barichivich, J., Briffa, K. R., & Sheffield, J. (2014). Global warming and changes in drought. *Nature Climate Change*, *4*, 17–22.

Wang, C., Liu, D., Luo, W., Fang, Y., Wang, X., Lü, X., Jiang, Y., Han, X., & Bai, E. (2016). Variations in leaf carbon isotope composition along an arid and semi-arid grassland transect in northern China. *Plant Ecology*, *9*, 576–585.

Wang, C., Wang, X., Liu, D., Wu, H., Lü, X., Fang, Y., Cheng, W., Luo, W., Jiang, P., Shi, J., Yin, H., Zhou, J., Han, X., & Bai, E. (2014). Aridity threshold in controlling ecosystem nitrogen cycling in arid and semi-arid grasslands. *Nature Communications*, *5*, 1–8.

Warton, D. I., Duursma, R. A., Falster, D. S., & Taskinen, S. (2012). SMATR 3—An R package for estimation and inference about allometric lines. *Methods in Ecology and Evolution*, *3*, 257–259.

Wittmer, M. H. O. M., Auerswald, K., Tungalag, R., Bai, Y. F., Schäufele, R., & Schnyder, H. (2008). Carbon isotope discrimination of C_3 vegetation in central Asian grassland as related to long-term and short-term precipitation patterns. *Biogeosciences*, *5*, 913–924.

Wright, I. J., Reich, P. B., & Westoby, M. (2001). Strategy shifts in leaf physiology, structure and nutrient content between species of high-and low-rainfall and high-and low-nutrient habitats. *Functional Ecology*, *15*, 423–434.

Wright, I. J., Reich, P. B., & Westoby, M. (2003). Least-cost input mixtures of water and nitrogen for photosynthesis. *The American Naturalist*, *161*, 98–111.

Wright, I. J., Reich, P. B., Westoby, M., Ackerly, D. D., Baruch, Z., Bongers, F., Cavender-Bares, J., & Chapin, T. (2004). The worldwide leaf economics spectrum. *Nature*, *428*, 821–827.

Zarovali, M. P., Yiakoulaki, M. D., & Papanastasis, V. P. (2007). Effects of shrub encroachment on herbage production and nutritive value in semi-arid Mediterranean grasslands. *Grass and Forage Science*, *62*, 355–363.

SUPPORTING INFORMATION

Additional supporting information can be found online in the Supporting Information section at the end of this article.

Figure S1. Map showing the 10 sampling locations (denoted by two letter codes) along a 350 km aridity gradient in the Iberian Peninsula.

Figure S2. Relationship between leaf $\delta^{18}O$ and K concentration for *Stipa tenacissima* individuals at 10 sampling locations along the aridity gradient.

Figure S3. Culm water $\delta^{18}O$ plotted against $\delta^{2}H$ values for *Stipa tenacissima* individuals at 10 sampling locations along the studied aridity gradient.

Table S1. Geographic and climatic characteristics of 10 sampling locations along the aridity gradient from Central to Southeastern Spain.

Table S2. Summary of mean (±SE), minimum and maximum values of *Stipa tenacissima* traits for pure-grass and shrub-encroached steppes at 10 sampling locations.

Table S3. Pearson's correlation coefficients between geographic and climatic variables of sampling locations along the aridity gradient ($n = 10$).

Table S4. Results from linear mixed regression models for relationships of *Stipa tenacissima* traits and PCA_{axis1} scores with key geographic and mean annual climatic variables across individuals along the aridity gradient.

Table S5. Results from linear mixed regression models for relationships of *Stipa tenacissima* traits and PCA_{axis1} scores with key mean seasonal climatic variables across individuals along the aridity gradient.

How to cite this article: Ren, W., García-Palacios, P., Soliveres, S., Prieto, I., Maestre, F. T., & Querejeta, J. I. (2024). Pushing the limits of C_3 intrinsic water use efficiency in Mediterranean semiarid steppes: Responses of a drought-avoider perennial grass to climate aridification. *Functional Ecology*, *38*, 955–966. https://doi.org/10.1111/1365-2435.14518